MARY KAY O'CONNOR PROCESS SAFETY CENTER
TEXAS A&M ENGINEERING EXPERIMENT STATION

22nd Annual International Symposium
October 22-24, 2019 | College Station, Texas

Effects of Non-uniform Blockage Ratio and Obstacle Spacing on Flame Propagration in Premixed H_2/O_2 mixtures

Cassio Brunoro Ahumada*[1], Eric L. Petersen[2], Qinsheng Wang[1]
[1]Artie McFerrin Department of Chemical Engineering, Texas A&M University, College Station, Texas, USA
[2]J. Mike Walker '66 Department of Mechanical Engineering, Texas A&M University, College Station, Texas, USA
*Presenter E-mail: cassioahumada@tamu.edu

Abstract

Most of the current research in flame propagation and deflagration-to-detonation transition (DDT), including large and small-scale experiments, have analyzed the influence of obstacles uniformly distributed on the explosion severity. These uniform conditions are characterized by constant obstacle spacing, shape and blockage ratio (BR), and may not represent very well the layout of actual industrial facilities. Therefore, the objective of this study was to investigate the effects of varied BR in the peak overpressure and flame acceleration. A systematic analysis was conducted by varying layout parameters on a regular basis to examine what conditions favor the highest overpressure and minimal run-up distance when DDT is observed. Experiments were performed in a closed pipe with 38 mm internal diameter and an overall length to diameter ratio (L/D) equal to 73. The arrangement between two obstacles in the test vessel was varied in terms of blockage ratio (increasing, decreasing and equal) and obstacle distance (1D, 2D, and 3D). From the conditions tested, the increasing blockage ratio has a more significant impact on the overall maximum pressure and the DDT run-up distance.

Keywords: Explosions, Vapor Clouds, DDT, Blast Effects

1. Introduction

Understanding flame propagation and explosion characteristics of flammable mixtures is crucial for industrial explosion protection of power plants and chemical plants. From the practical point of view, safety professionals work towards estimating flame speeds and maximum overpressure build-up for a wide range of industrial releases scenarios. This information

is later used to support safety design decisions and protective measure specifications. Defining the entire spectrum of plausible scenarios is not a straightforward task, it must address all affecting parameters including release locations, mixture concentration, the volume of flammable cloud, equipment density and disposition, and ignition position. This problem can be simplified by identifying and ranking conditions that are likely to lead to more severe explosion cases.

For several years it has been known that the presence of obstructions can give rise to substantial overpressure during combustion of premixed flammable gases[1, 2] . Therefore, researchers have proposed empirical correlations[3, 4] and numerical codes [5-7] to account for obstruction characteristics (equipment density and spacing) during explosion modeling analysis. Despite their usefulness, the majority of these methods were validated against uniform obstruction conditions that were far from the non-ideality encountered in industrial facilities. Such uniformity can be characterized by multiple obstacles with similar shapes and blockage ratio, distributed at equally spacing inside a combustion chamber, and may not be very representative on the actual industrial facilities layout.

To put into perspective, the authors created an obstacle complexity index (OCI) that can be estimated based on four factors: obstacle shape, BR, obstacle spacing, and uniformity. The following expression can be used to quantify OCI:

$$OCI = \prod_{i=1}^{4} F_i$$

Where

$$F_i = [1,3]$$

Table 1. Value for obstacle factor (F_i) based on test conditions.

Factor Value (F_i)	Obstacle Shape	Obstacle Spacing	Blockage Ratio	Number of different obstacles
1	Tests without obstacles	Tests without obstacles	Tests without obstacles	Tests without obstacles
2	Round obstacles (orifice plates and cylinders)	Tests with equally spaced obstacles	Continuous BR	At least 2
3	Obstructions with sharp edges	Tests with varied obstacle spacing	Varied BR	More than 2

Table 1 contains more detail on each factor value. Figure 1 shows the relationship between the flammable mixture volume and OCI of experiments listed in the literature. It can be observed that most of the industrial explosions are located in the upper-right quadrant, which represents the high complexity and large volume region; whereas the majority of the work on the literature are placed on the lower quadrants, including small and large volume regions with the exception of

limited tests with propane and methane mixtures[8, 9]. In the later cases, authors analyzed the efficiency of venting panels on explosion mitigation inside obstructed enclosures simulating offshore installations. Although insightful observations on the effects of obstacle congestion in large-scale tests were obtained, only three distinct sets of layout displacement were studied giving limited conclusions on the influence of obstacle orientation and geometry.

The round points in red represent the capabilities of the current facility based on previous works [10, 11]. Even though the mixture volume is considerably lower than the ones experienced during an industrial explosion, our aim to towards understanding in more detail how obstacle characteristic play a role in turbulent combustion propagation and detonation onset. For that purpose, it is fundamental to conduct experiments in a controllable test environment. The data generated by this work can be used for validation purposes of current numerical models.

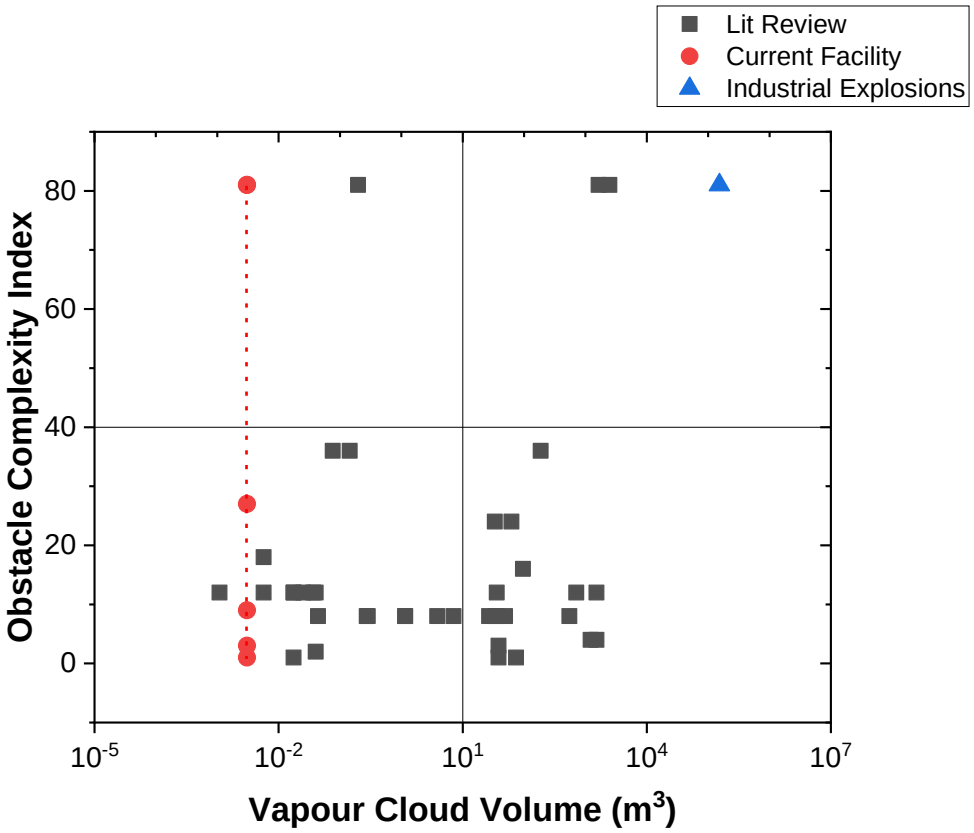

Figure 1. Variation of obstacle complexity index with flammable mixture volume

2. Experimental Details

Experiments were carried out in a horizontal tube with a length of 2.77 m and a 38-mm internal diameter, as shown in Figure 2. The tube is closed at both ends, and ignition was via a low-voltage, automotive glow plug operated at 10 A positioned centrally at the left-endplate. An expansion volume is located at the end-wall opposed to the ignition point, enabling the use of multiple spacers with different widths. A spacer with 25.4-mm width was maintained during all

tests to minimize disturbances from reflected shocks propagating ahead of the flame. The pressure was recorded at seven different locations along the tube (P1 to P7) using piezoelectric pressure transducers, PCB 113B22, with a measurement range of 34.5 MPa, a rise time smaller than 1 μs, and a resonance frequency ≥ 500 kHz. Data were recorded using a PC oscilloscope board (GaGeScope) at a sampling rate of 1 MS/s.

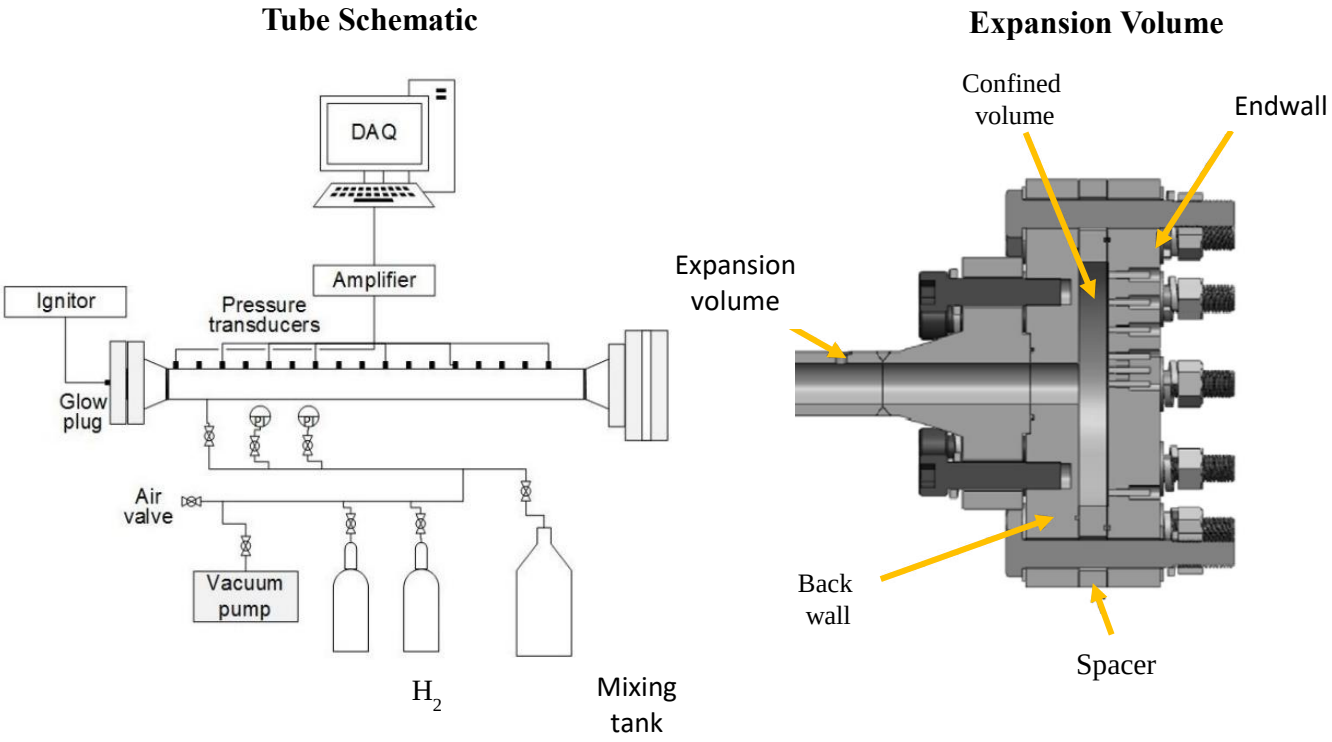

Figure 2. Schematic of the detonation tube utilized during experiments (left side) and the expansion volume located at endwall (right side)

All tests were conducted at ambient temperature, roughly 20°C. Stochiometric hydrogen/oxygen mixtures were prepared by the method of partial pressures in a separate mixing tank and left overnight. Two ring-shaped obstacles with 5-mm thickness were used during each test, with the first obstacle fixed at a distance of 80 mm from the ignition point. The arrangement between obstructions in the test vessel was changed in terms of blockage ratio (increasing, decreasing, and equivalent) and obstacle separation distance (38, 76, and 114 mm). Table 2 summarizes all conditions tested in this study. A full factorial design was conducted, resulting in 27 different experimental conditions. Each experimental condition was repeated at least three times. Figure 3 depicts obstacle shapes and displacement inside the tube during experiments.

Table 2. Summary of Experimental Conditions

Variable	Level 1	Level 2	Level 3
1st Obstacle BR	25%	40%	80%
2nd Obstacle BR	25%	40%	80%
Obstacle Spacing	38 mm	76 mm	114 mm

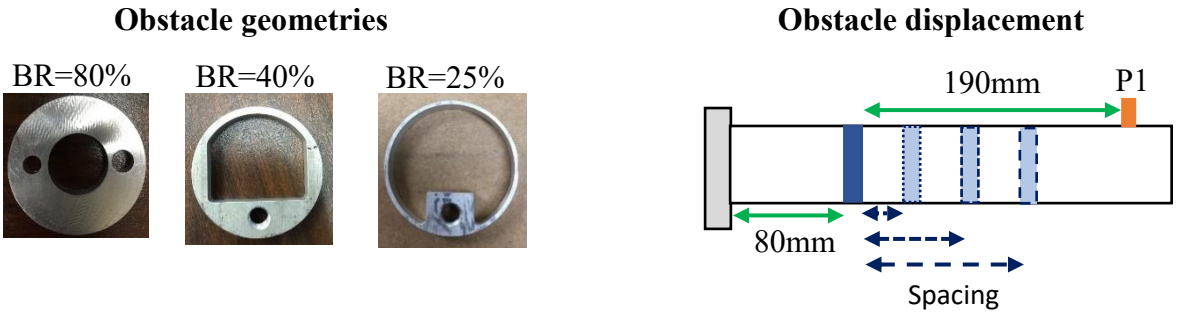

Figure 3. Illustration of the obstacles inserted inside the detonation tube.

3. Results and Discussion

3.1. Facility Characterization

A facility characterization study was performed with the tube emptied to analyze flame propagation without the presence of obstacles at initial pressure ranging from 30 to 300 Torr. Figure 4 shows the variation of the maximum shock wave speed (on the left) and the DDT time (on the right) with initial pressure. It can be observed that mixtures with initial pressure above 60 Torr experienced DDT whereas mixtures below 50 Torr did not ignite. Another interesting observation is the reduction in time when DDT was first identified in the facility – DDT time.

Figure 5 and 6 depict the overpressure profile with time along the tube at 50 and 150 Torr, respectively. Both cases experienced a leading shock wave traveling toward the right-end plate are observed, indicating an initial flame acceleration. For 150 Torr, a rapid transition to detonation takes place in the second half of the tube (between P10 and P13) creating overpressures around 4 bars. At 50 Torr (Figure 5), the precursor shock velocity remained above the sound speed at the reactants (540 m/s) but below the sonic velocity on the combustion products (~1,000 m/s). This is the characteristics of the “choke regime” [12]. Although flame arrival time was not measured directly, it can be inferred from the leading shock velocity profile that flame speed was near the local sound speed. The increase in shock velocity in the first half of the tube indicates that a flame front is propagating jointly behind the pressure front, forming a flame-shock structure.

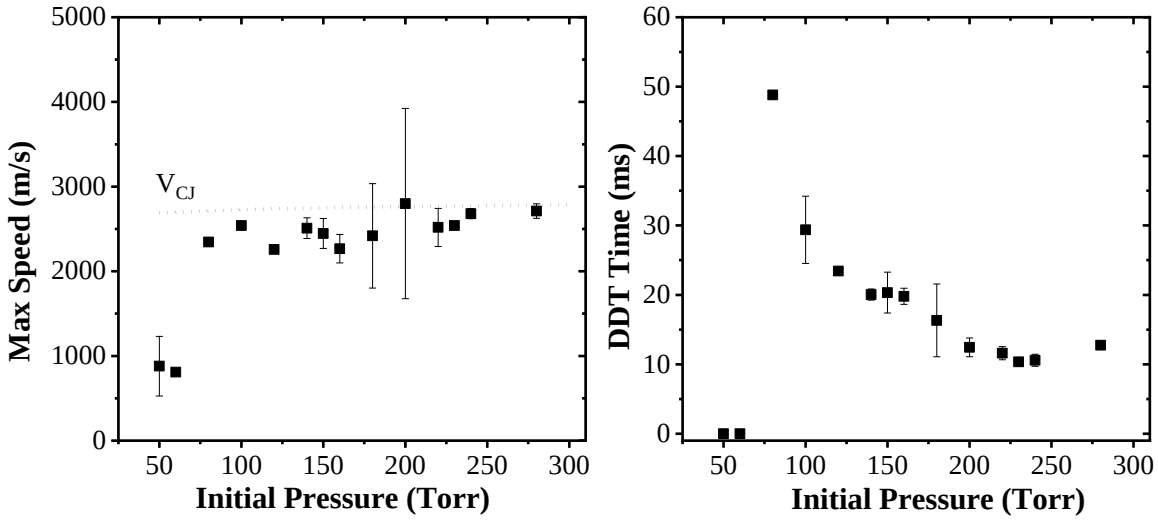

Figure 4. Variation of the maximum shock wave speed (on the left) and the DDT time (on the right) with initial pressure.

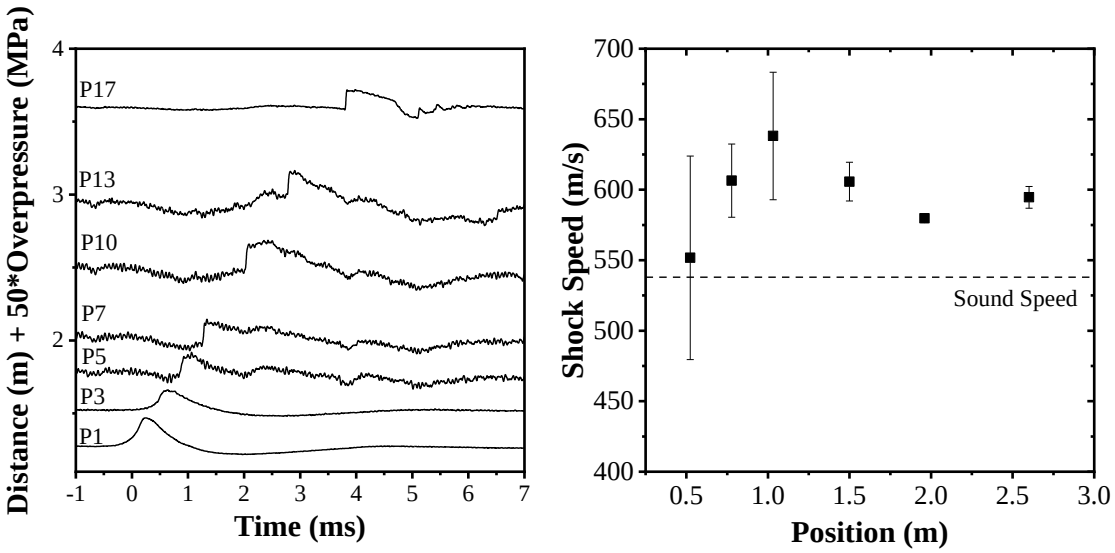

Figure 5. Pressure results obtained for a stoichiometric hydrogen-oxygen mixture initially at 50 Torr and with the tube emptied. Pressure is normalized by side-on pressure measured (MPa) multiplied by 50 and added the pressure sensor distance (m).

On the other hand, the mixture initially at 150 Torr demonstrates an entirely different behavior. An early acceleration creates a series of sonic waves traveling towards the right-endplate. Then, a rapid transition to detonation takes place in the second half of the tube (between P10 and P13). Even though DDT was not expected given the size of the internal tube diameter, the preceding waves increase the initial temperature of reactant mixture, increasing the reactivity of the mixture and propensity to detonation onset.

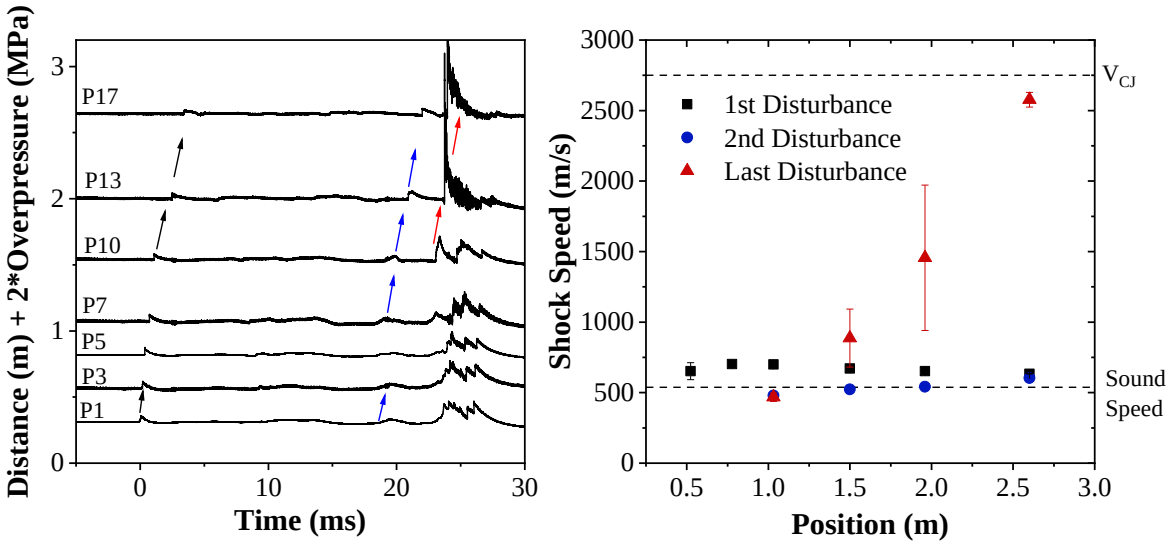

Figure 6. Pressure results obtained for a stoichiometric hydrogen-oxygen mixture initially at 150 Torr and with the tube emptied. Pressure is normalized by side-on pressure measured (MPa) multiplied by 2 and added the pressure sensor distance (m).

The facility characterization study showed that fast deflagrations and DDT are observed at the current set-up, The next section contains the results for the mixture at 150 Torr. Experiments with 50 and 100 Torr were completed, but at the current stage data analysis is still in progress and, therefore, will not be shown in this report.

3.2. Results for $H_2 + O_2$ mixtures at 150 Torr

After confirming that DDT is possible even with the absence of obstacles, experiments were carried out to investigate the effects of varied blockage on the explosion characteristics. As expected, deflagration-to-detonation transition was observed in all 27 experimental cases, but at different locations. Figure 7 shows the variation of maximum overpressure at the first sensor (P1) with average BR. Similar to the uniform condition case, Pmax increases as averaged BR changes from 0 to 60 %, most likely due to higher turbulence intensities. Then as BR changes to 80%, momentum losses become significant leading to a reduction in Pmax. One interesting observation is for the case of 40%-80% BR separated at 76 mm (2 internal diameters), in which detonation occurred before P1, reducing the run-up distance considerably. A possible explanation for the early detonation onset can be the reflection of the shock induced by the obstacle in the confinement wall as reported by Obara et al. [13]. Another reason could be the accumulation of multiple Mach stems generated by local explosions triggered by turbulent jet combustion near the confinement walls; this accumulation process creates stronger shocks that can trigger a detonation in hot-spots via shock focusing [14]. Currently, the absence of optical windows limits our ability for a detailed understanding of mechanisms behind detonation onset for this particular case. However, this behavior is very intriguing given that DDT was achieved using only two obstacles.

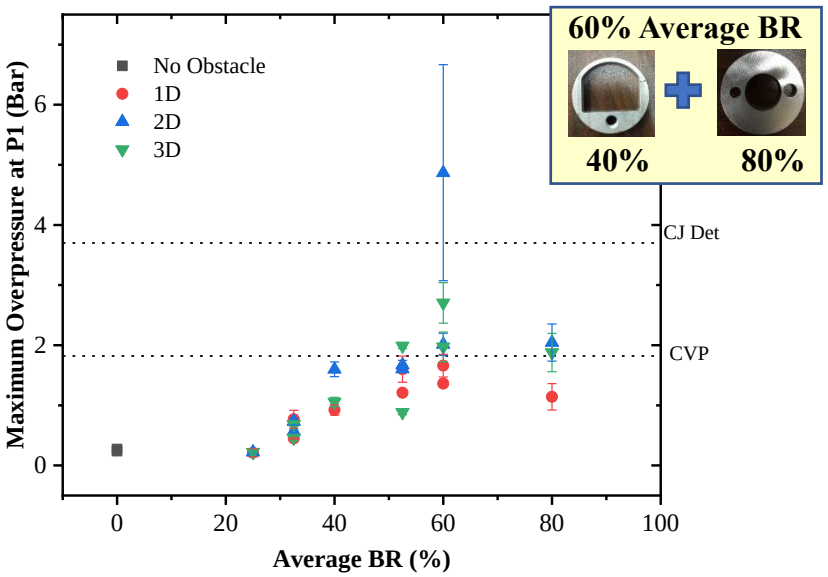

Figure 7. Variation of maximum overpressure with average BR at first pressure sensor (P1) in the wake of second obstacle.

In overall, four general propagation behaviors were identified (see Fig. 8) based on the time between the leading wave and the onset of DDT. In case I, a preceding wave continuously accelerates until it reaches a final speed near the Chapman-Jouguet detonation. This case can be further divided into two, I-A and I-B. The former, as mentioned earlier, consists of a strong shock that is created in the wake of the second obstacle and is detected early by sensor P1 or P3 located at 190 mm and 460 mm from the 1st obstacle, respectively. Since the detonation onset occurs earlier, there is no sign of retonation propagating backward towards the ignition point. In the case of I-B, DTT takes place within the second half of the tube near the leading shock front. For combustion type II, a shock wave is formed and accelerated up to speeds of 1500 m/s in the first half of the tube and later decelerated to final speeds around 800 m/s towards the closed end. The leading wave is not strong enough to ignite the mixture via shock compression and, as a result, the onset of DDT takes places after it passes. This behavior is typical for conditions when detonation onset occurs on the turbulent flame brush [15]. Case III is very similar to case II; however, in Case III, two major pressure waves are observed before the transition to detonation. The fact that the second pressure front is accelerating indicates that a flame-shock structure is formed and that detonation takes place after the flame passes. Gaathaug *et al.* [14] reported a similar phenomenon that was caused due to shock accumulation resulting from multiple local explosions. In case IV, on the other hand, numerous pressure waves are formed and travel near the sonic velocity in the medium; this indicates a slow flame acceleration followed by a sudden transition that takes place towards the end of the tube.

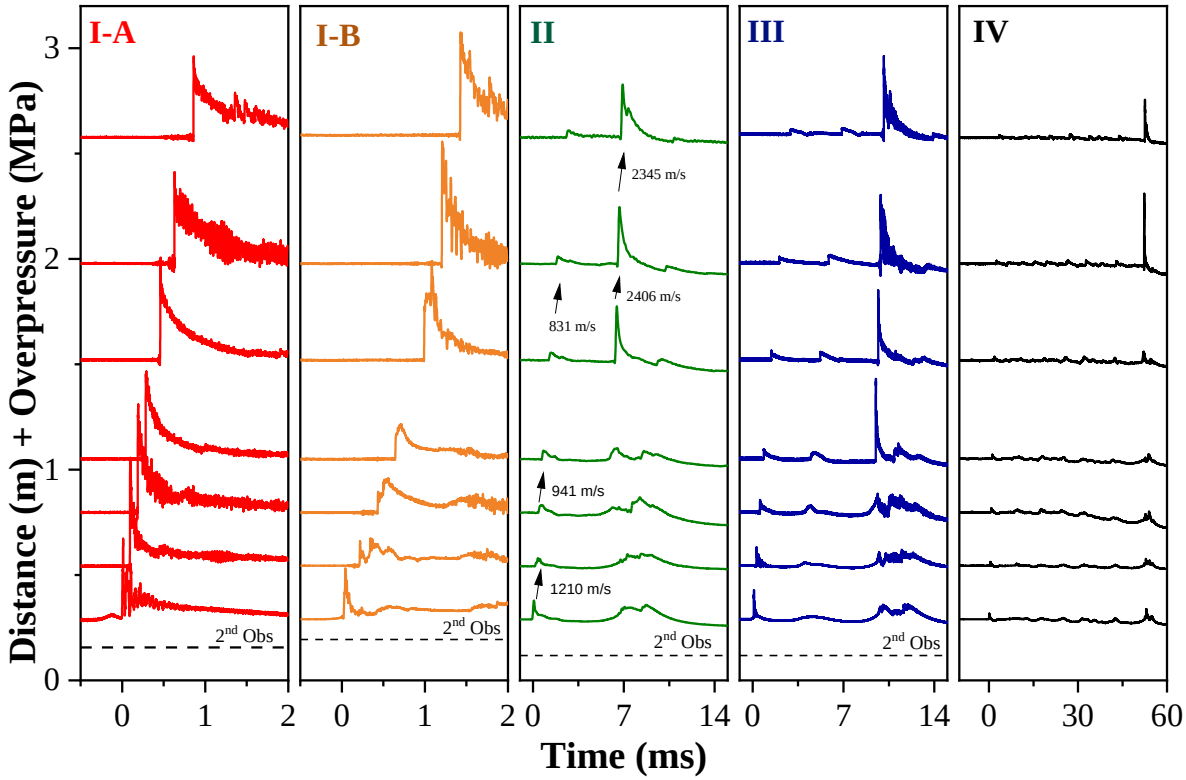

Figure 8. Representation of the four different types of combustion propagation behaviors identified.

Table 3 summarizes the predominant propagation behavior for each condition tested. The most robust combustion regime (Case I) occurred for obstructions with a higher blockage in the second obstacle (80-80, 40-80, and 25-80). It is reasonable to assume that narrower obstruction gaps may generate faster and stronger shocks as the flame front passes the solid obstruction. This strong shock can ultimately lead to detonation onset. Another important aspect is the distance between the obstacle and the ignition point — longer spacing results in faster flames before reaching the obstacle surface. For instance, cases with higher BR closer to ignition (80-40 and 80-25) resulted mostly combustion type III, in which leading shock front was significantly lower.

Table 3. Summary of prevailing propagation conditions for obstacle characteristic

		Obstacle Spacing		
Blockage Distribution	**Average ABR**	**1D**	**2D**	**3D**
80-80	80%	II	I-B	I-B
80-40	60%	III	III	I-B
40-80	60%	II	I-A	I-A
80-25	53%	III	III	III
25-80	53%	I-B	I-B	I-B
40-40	40%	III	II	II
40-25	33%	III	III	II

25-40	33%	II	III	III
25-25	25%	III	II	III
No obstacle	0%	IV	IV	IV

Another interesting observation is that obstacle pairs with the same average blockage ratio resulted in distinct combustion characteristics, especially when BR variation was more abrupt. For instance, comparing the results from the obstacle pair 40-80 with its equivalent on average blockage (but transposed), 80-40, one may observe that the increasing obstruction leads to a stable detonation within the first three sensors (see Figure 9). Conversely, in the decreasing blockage case, DDT takes place mostly within the second half of the tube (after P4), and it is preceded by two major pressure waves. Similar conclusions were obtained for obstacle pairs 80-25 and 25-80. Contrarily, obstacle pairs with smoothers changes in BR (40-25, 25-40) in general did not demonstrate significant differences in behavior.

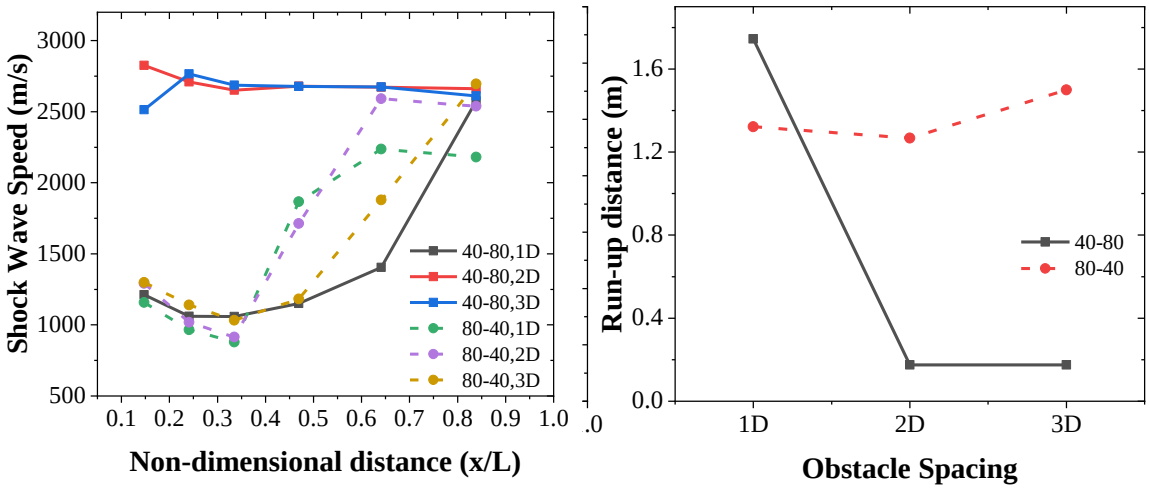

Figure 9. Comparison between obstacle pairs with an equivalent average blockage ratio.

Based on this study, we can conclude that the obstacle order does affect flame propagation and explosion severity for such high sensitivity mixture. This effect is more significant when a high degree of obstruction is present. For instance, for the 60% average BR case, the run-up distance was much shorter when 80% BR obstacle was locater after the 40% BR obstacle. Conversely, switching the obstruction displacement to 80-40 lead to longer run-up distances. This indicates that obstruction geometry should be considered when more than one obstruction shape is present and that looking only at the average BR may lead to underestimated results. The authors acknowledge that this is a preliminary result and further analysis will be conducted to investigate the isolated impact of obstacles with varied BR and similar shapes as well as obstacles with distinct shapes but identical BR.

4. Concluding Remarks

Experiments on flame propagation and DDT were carried out in stoichiometric, premixed hydrogen-oxygen mixtures at 150 Torr in a closed tube with two obstacles of varying configuration. Round-shaped obstacles with three different blockages (25%, 40%, and 80%) were used, and the arrangement between the obstacles was changed in terms of blockage distribution (increasing, decreasing, and equivalent) and obstacle distance (1D, 2D, and 3D). Four distinct propagation behaviors were identified based on the time between the leading wave and the onset of DDT. From the conditions tested, obstacle pairs with a higher blockage in the second obstruction lead to strong combustion. It was observed that obstructions with equivalent blockage resulted in distinct propagation characteristics and explosion strength. This study is still in progress, and additional experiments will be conducted to understand the mechanisms underlining these different behaviors.

References

[1] W. R. Chapman and R. V. J. J. o. t. C. S. Wheeler, "VI.—The propagation of flame in mixtures of methane and air. Part V. The movement of the medium in which the flame travels," pp. 38-46, 1927.

[2] I. O. Moen, "Transition to detonation in fuel-air explosive clouds," *Journal of Hazardous Materials,* vol. 33, no. 2, pp. 159-192, 2// 1993, doi: http://dx.doi.org/10.1016/0304-3894(93)85052-G.

[3] A. J. Pierorazio, J. K. Thomas, Q. A. Baker, and D. E. Ketchum, "An update to the Baker-Strehlow-Tang vapor cloud explosion prediction methodology flame speed table," *Process Safety Progress,* vol. 24, no. 1, pp. 59-65, 2005, doi: 10.1002/prs.10048.

[4] S. Dorofeev. "Flame acceleration and ddt: A framework for estimating potential explosion hazards in hydrogen mixtures." http://www.hysafe.org/science/eAcademy/docs/3rdesshs/presentations/ESSHS2008DorofeevSB.pdf (accessed 2016).

[5] B. Hjertager, K. Fuhre, S. Parker, J. J. P. i. a. Bakke, and aeronautics, "Flame acceleration of propane-air in a large-scale obstructed tube," vol. 94, pp. 504-522, 1984.

[6] O. R. Hansen and D. M. Johnson, "Improved far-field blast predictions from fast deflagrations, DDTs and detonations of vapour clouds using FLACS CFD," *Journal of Loss Prevention in the Process Industries,* vol. 35, pp. 293-306, 5// 2015, doi: http://dx.doi.org/10.1016/j.jlp.2014.11.005.

[7] G. Ciccarelli, C. T. Johansen, and M. Parravani, "The role of shock–flame interactions on flame acceleration in an obstacle laden channel," *Combustion and Flame,* vol. 157, no. 11, pp. 2125-2136, 2010, doi: 10.1016/j.combustflame.2010.05.003.

[8] B. Hjertager, K. Fuhre, and M. J. J. o. l. p. i. t. p. i. Bjørkhaug, "Gas explosion experiments in 1: 33 and 1: 5 scale offshore separator and compressor modules using stoichiometric homogeneous fuel/air clouds," vol. 1, no. 4, pp. 197-205, 1988.

[9] C. Selby and B. J. S. p. Burgan, "Blast and fire engineering for topside structures-phase 2: final summary report," 1998.

[10] C. A. Rosas Martinez, "Deflagration-to-Detonation Transition (DDT) Studies: Effect of Non-Uniform Obstacle Distribution on DDT," Doctoral, Material Science Texas A&M University, Internal report, 2016.
[11] N. L. Polley, M. Q. Egbert, and E. L. Petersen, "Methods of re-initiation and critical conditions for a planar detonation transforming to a cylindrical detonation within a confined volume," *Combustion and Flame*, vol. 160, no. 1, pp. 212-221, 2013/01/01/ 2013, doi: https://doi.org/10.1016/j.combustflame.2012.09.017.
[12] J. H. Lee, R. Knystautas, and C. K. Chan, "Turbulent flame propagation in obstacle-filled tubes," *Symposium (International) on Combustion*, vol. 20, no. 1, pp. 1663-1672, 1985/01/01/ 1985, doi: https://doi.org/10.1016/S0082-0784(85)80662-7.
[13] T. Obara, T. Kobayashi, and S. Ohyagi, "Mechanism of deflagration-to-detonation transitions above repeated obstacles," *Shock Waves*, vol. 22, no. 6, pp. 627-639, 2012, doi: 10.1007/s00193-012-0408-5.
[14] A. V. Gaathaug, D. Bjerketvedt, and K. Vaagsaether, "Experiments with Flame Propagation in a Channel with a Single Obstacle and Premixed StoichiometricH2-Air," *Combustion Science and Technology*, vol. 182, no. 11-12, pp. 1693-1706, 2010, doi: 10.1080/00102202.2010.497355.
[15] G. Ciccarelli and S. Dorofeev, "Flame acceleration and transition to detonation in ducts," *Progress in Energy and Combustion Science*, vol. 34, no. 4, pp. 499-550, 8// 2008, doi: http://dx.doi.org/10.1016/j.pecs.2007.11.002.